NÖHÜ Müh. Bilim. Derg. / NOHU J. Eng. Sci., 2025; 14(1), 360-369

Niğde Ömer Halisdemir Üniversitesi Mühendislik Bilimleri Dergisi
Niğde Ömer Halisdemir University Journal of Engineering Sciences

Araştırma makalesi / Research article

www.dergipark.org.tr/tr/pub/ngumuh / www.dergipark.org.tr/en/pub/ngumuh

The effect of air-cooling heat treatment on the microstructure and phase transformations of structural steels

Yapı çeliklerinin mikroyapısı ve faz dönüşümleri üzerine hava soğutmalı ısıl işlemin etkisi

Semih Mahmut Aktarer[1, *]

[1] *Recep Tayyip Erdogan University, Department of Automotive Technology, 53020, Rize, Türkiye*

Abstract

The aim of this study was to investigate the microstructure, phase transformations, and hardness changes of S235JR, S275JR, and S355JR structural steels after air-cooled heat treatment. The steel samples were austenitized at 1000°C and then cooled in air, and the sample temperatures were recorded with a thermocouple during cooling. The microstructure and phase transformations of the samples were analyzed both experimentally and with the Computerized Combining Phase Diagrams and Thermochemistry (CALPHAD) material property software. It was observed that higher carbon and manganese levels in structural steels lower the phase transformation temperatures, promote bainite formation, reduce the average ferrite grain size, and consequently lead to an increase in hardness. The phase ratios and hardness values were determined by the predicted experimental results with a deviation of less than 3%. These results show that a balanced ferrite and bainite phase distribution is achieved air cooling and the software effectively models these transformations.

Keywords: Structural steels, Air cooling, Microstructure, Phase transformation, CALPHAD

Öz

Bu çalışmanın amacı, S235JR, S275JR ve S355JR yapısal çeliklerinin hava soğutmalı ısıl işlem sonrası mikro yapısını, faz dönüşümlerini ve sertlik değişimini incelemektir. Çelik numuneleri, 1000°C'de östenitleştirdikten sonra havada soğutulmuş ve soğuma esnasında numune sıcaklıkları bir termokupl ile kaydedilmiştir. Numunelerin mikro yapı incelemeleri ile faz dönüşümleri hem deneysel yöntemlerle hem de Faz Diyagramlarının ve Termokimyanın Bilgisayarla Birleştirilmesi (CALPHAD) malzeme özelliği yazılımıyla analiz edilmiştir. Yapı çeliklerinde artan karbon ve mangan içeriği faz dönüşüm sıcaklıklarını düşürerek beynit oluşumunu arttırdığı, ferrit ortalama tane boyutunu küçülttüğü ve bu yüzden de sertlik değerlerinde artışa yol açtığı görülmüştür. Yazılım ile belirlenen faz oranları ve sertlik değerleri, deneysel sonuçları %3'ten düşük bir sapma ile tahmin etmiştir. Bu sonuçlar, hava soğutma ile dengeli bir ferrit ve beynit faz dağılımının elde edildiğini ve malzeme özellik yazılımının bu faz dönüşümlerini başarılı bir şekilde modelleyebildiğini göstermektedir.

Anahtar kelimeler: Yapısal çelikler; Havada soğutma, Mikroyapı, Faz dönüşümü, CALPHAD

1 Introduction

Structural steel is widely preferred in many industries, especially in construction and machinery, thanks to their high strength, good weldability, formability and cost-effectiveness [1]. Especially in the automotive industry, their use in chassis parts, body panels and other structural components stands out [2]. The preference of these steels in the automotive sector increases the durability of vehicles, while at the same time contributing to fuel efficiency by optimizing weight [1]. Structural steels are classified as carbon-manganese steels and their microstructure, which can be modified by heat treatment, allows mechanical properties to be easily improved [3]. Numerous studies have been carried out to improve the performance and environmental resistance of structural steels. Solomon et al. [4] investigated the synergistic effects of additives such as poly in mitigating chloride-induced dissolution in S235JR steel, thereby contributing to corrosion protection. Similarly, Krella et al. [5] investigated the cavitation erosion resistance of S235JR, shedding light on its durability under dynamic fluid conditions. Mechanical properties were a key focus. Irsel [6] analysed microstructural and mechanical relationships in S235JR steel using different welding techniques, while Gamerdinger et al. [7] investigated tensile strength in laser-welded seams, demonstrating the benefits of advanced welding technologies. Fatigue performance and fracture mechanisms have also been extensively investigated. Neimitz and Galkiewicz [8] conducted experimental and numerical analyses of fracture mechanisms in S355JR steel, while Torić et al. [9] developed a high-temperature material model for S275JR steel, advancing knowledge of extreme state behaviour. Efforts to improve corrosion resistance are noteworthy. Chen et al. [10] investigated residual stresses in welded joints between S355JR and stainless steel, while Yongzhong et al. [11] improved the corrosion resistance of S275JR using amorphous AlCrNi coatings. Collectively, these studies highlight significant advances in structural steel research, particularly in corrosion resistance, mechanical

* Sorumlu yazar / Corresponding author, e-posta / e-mail: semih.aktarer@erdogan.edu.tr (S. M. Aktarer)
Geliş / Recieved: 04.11.2024 Kabul / Accepted: 29.12.2024 Yayımlanma / Published: 15.01.2025
doi: 10.28948/ngmuh.1578719

properties and durability under different loading conditions. These research advancements not only contribute to improved processing and alloy design strategies but also emphasize the critical role of microstructural control in structural steels. This plays a critical role in meeting the safety and performance requirements of the construction, machinery and automotive industries. The martensitic microstructure of structural steels after rapid cooling results in high hardness but low ductility, which is undesirable in terms of strength-toughness balance [12]. Overly hard structures can negatively impact mechanical performance by raising the likelihood of brittle fractures in applications [13]. Therefore, controlled slow cooling enables the gradual development of phases such as ferrite, bainite, and pearlite, promoting a well-balanced microstructure [14]. Bainitic microstructures provide an optimal combination of strength and toughness, especially for large components where consistent rapid cooling is unfeasible. These microstructural attributes are widely utilized in sectors such as defense, nuclear, and automotive industries [14]. Recent research has explored how slow cooling rates and various heat treatment techniques influence the microstructure and strength of steels, aiming to enhance their mechanical properties. Chakraborty et al. [14] highlighted the potential for producing carbide-free bainitic steel by showing that slow cooling rates can promote bainitic microstructure formation in low-carbon steels. Ding et al. [15] found that slow cooling rates in Q420 and Q690 steels significantly reduced strength but enhanced ductility. Di Martino and Thewlis [16] investigated the transformation characteristics of ferrite/carbide aggregates (FCA) in low-carbon manganese steels, showing that this structure forms at rates similar to those of Widmanstätten ferrite. These studies collectively demonstrate how microstructural transformations and heat treatment parameters influence steel properties. Thakur and Aregawi [17] examined the potential for improving the mechanical properties of ST 37-2 steel by heat treatments and found that treatments such as quenching and tempering increase strength and hardness, while annealing increases ductility. Fadare et al. [2] emphasized that NST 37-2 steel can be optimized by heat treatments and especially hardening provides high strength and hardness. Finally, Dobrzański and Honysz [13] stated that air cooling is an effective method to obtain stable mechanical properties, but gives lower results in terms of hardness compared to quenching.

The research above shows how different heat treatments influence both the microstructure and the mechanical characteristics of steel. Forming ferritic and bainitic structures is an important approach to optimizing strength and ductility, especially in low-carbon steels. Although much research has been done on the rapid cooling of steels (e.g. quenching), there is a need for studies on the effects of air cooling on phase transformations and mechanical properties. Cooling at slow and moderate rates aids in forming ferritic and bainitic structures in steels, leading to optimal strength and ductility, reducing internal stresses, eliminating the need for additional heat treatment, and lowering energy costs. Consequently, further studies are required to examine the effects of air cooling on microstructure and mechanical characteristics, particularly in low-carbon steels. In this study, the microstructural attributes, phase transformations, and hardness levels of S235JR, S275JR, and S355JR structural steels subjected to air cooling were analyzed and compared with computational material modeling software results.

2 Experimental procedure

The chemical compositions of the structural steels investigated in the current study are presented in Table 1. Specimens with dimensions of 25 × 25 × 3 mm were prepared from commercially available plates. These specimens were kept in a box-type resistance furnace at 1000 ºC for 30 minutes and then cooled in air. To ensure the complete austenitization of the steel sample of this size and to achieve a homogeneous initial microstructure, the existing heat treatment parameters have been determined from the literature [2,13,16]. The temperature of the samples during cooling in air was recorded using a K-type thermocouple. The cooling rate was calculated from temperature data between 800ºC-500ºC, the range in which critical phase transformations can be observed in steel before martensite formation [16,18]. The specimens were first sanded step by step with sandpaper from 400 grit to 1500 grit and then polished with a 1 µm diamond suspension. In order to reveal the microstructural details, the specimens were etched with 2% Nital (2 ml HNO_3 + 98 ml C_2H_6O) solution for 15 seconds. Microstructure images of the specimens were examined with an optical microscope and quantitative microstructure measurements were performed using ImageJ software. Phase fractions were determined by histogram thresholding method and grain size properties were determined based on linear intercept method. JMatPro, a Java-based commercial software was used to calculate Time-Temperature Austenitization (TTA), Time-Temperature Transformation (TTT), and Continuous Cooling Transformation (CCT) diagrams. JMatPro models ferrite, pearlite, and bainite transformations in steels, closely following the principles of the Kirkaldy model [19,20]. Hardness was measured using a Vickers microhardness tester, applying a 300 g load for a duration of 10 seconds.

Table 1. Shows the given chemical composition of structural steels used in the current study

Samples	Chemical composition (wt.%)							
	C	Mn	P	S	Si	Cu	N	Fe
S235JR	0.10	0.61	0.023	0.022	0.18	0.24	0.012	Balance
S275JR	0.16	0.78	0.025	0.017	0.20	0.31	0.012	Balance
S355JR	0.21	1.12	0.030	0.030	0.24	0.45	0.012	Balance

3 Results and discussion

The optical microstructures, phase fractions and grain size distribution graphs of the structural steels used in this study are presented in Figure 1. In optical microscope images, ferrite appears gray, and pearlite appears black. In the phase maps, ferrite is highlighted in gray and pearlite in red after thresholding. S235JR steel shows an equiaxed

ferritic microstructure with relatively small pearlite islands distributed throughout the ferrite matrix (Figure 1(a)-(a1)). The pearlite phase fraction in this steel was 12% (Figure 1(a2)) and the average grain size of ferrite was measured to be approximately 7.92 µm (Figure 1(a3)). In S275JR steel, the average grain size of ferrite was 7.88 µm and the pearlite phase fraction was 22% (Figure 1(b)-(b3)). S355JR steel has an average ferrite grain size of 9.05 µm and exhibits a banded microstructure with a pearlite fraction of 30% (Figure 1(c)-(c3)). The microhardness values of S235JR, S275JR and S355JR steels were 140 $HV_{0.3}$, 165 $HV_{0.3}$ and 185 $HV_{0.3}$ respectively. The hardness of structural steels increases with increasing pearlite fraction. There is no significant difference between the average grain sizes of S235JR and S275JR, which are slightly smaller than those of S355JR. Therefore, the grain size effect on the hardness of the three structural steels is quite low compared to the pearlite phase fraction.

Figure 2 shows the temperature dependent phase transformations of ferrite, pearlite and austenite in S235JR, S275JR and S355JR structural steels. The phase fractions at room temperature were calculated as 86.2% ferrite and 13.8% pearlite for S235JR, 78.4% ferrite and 21.6% pearlite for S275JR and 71.9% ferrite and 28.1% pearlite for S355JR. These values, derived using JMatPro software, deviate by no more than 2% from the experimentally observed phase distributions presented in Figure 1.

TTA diagrams presented in Figure 3 compare the austenitization behavior of S235JR, S275JR and S355JR steels at different heating rates. In the diagrams, it is seen that the austenite starts temperature (A_1), austenite end temperature (A_3) and homogenization temperatures of the austenite phase vary according to the steel types. An upward trend was observed in these temperatures with an increasing heating rate. For S235JR, S275JR and S355JR steels, A_1 temperatures were 709°C, 709°C and 705°C; A_3 temperatures were 858°C, 833°C and 810°C; and homogenization temperatures of austenite were 887°C, 870°C and 858°C at 1°C/s heating rate, respectively Among these, S235JR steel exhibits higher A_1 and A_3 temperatures than the other structural steels, due to its lower carbon and manganese content. Although the A_1 temperature of S275JR remains constant, its A_3 temperature is lower. S355JR steel, with a higher carbon and manganese content, has lower. Figure 4 presents TTT diagrams calculated using JMatPro software for structural steels S235JR, S275JR and S355JR. These diagrams provide important information about the isothermal phase transformation behavior of steels and reveal how this behavior is influenced by the chemical composition of the steels concerned. The ferrite transformation temperature of 235JR, S275JR and S355JR

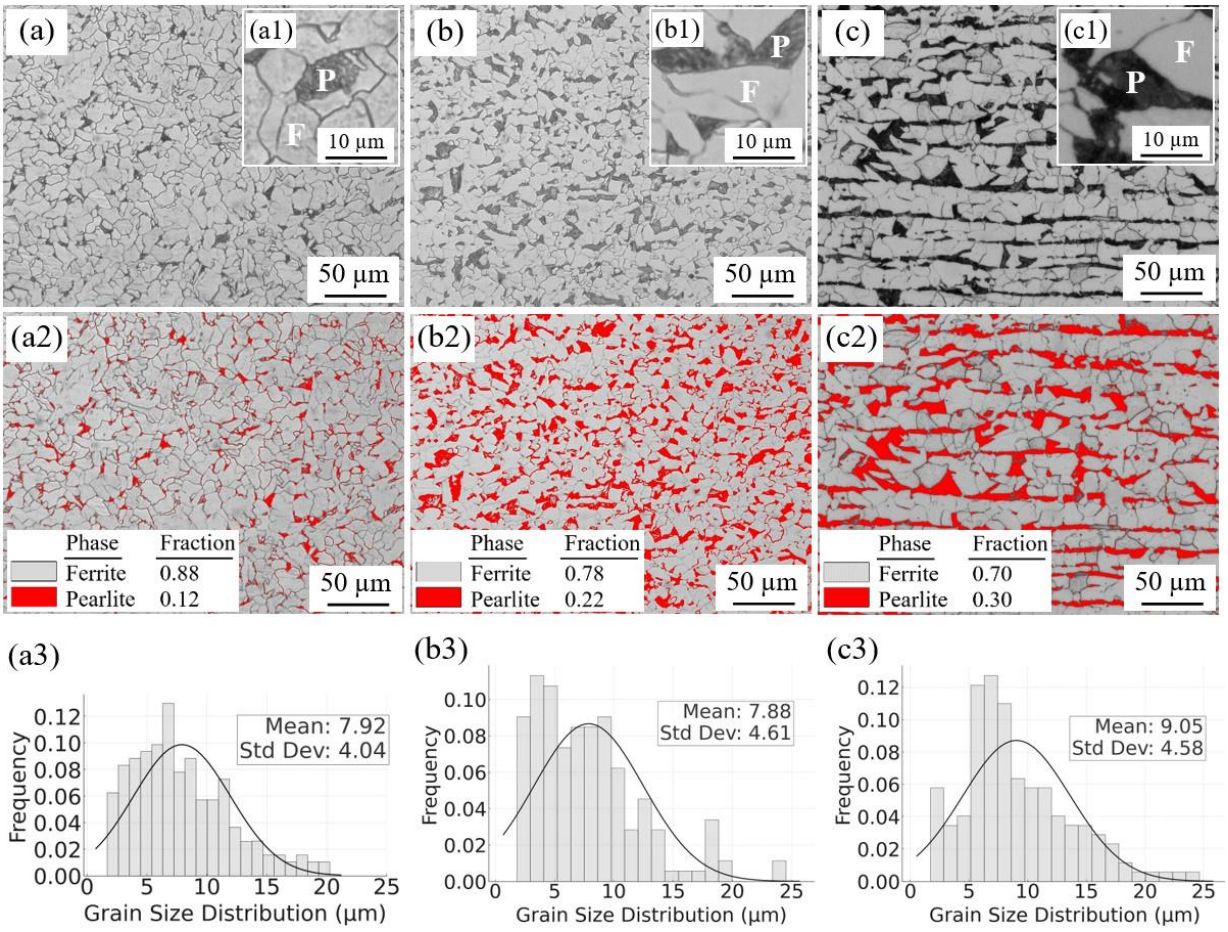

Figure 1. Optical microscope images, phase maps, and grain size distributions of the initial microstructures of (a)-(a3) S235JR, (b)-(b3) S275JR, and (c)-(c3) S355JR

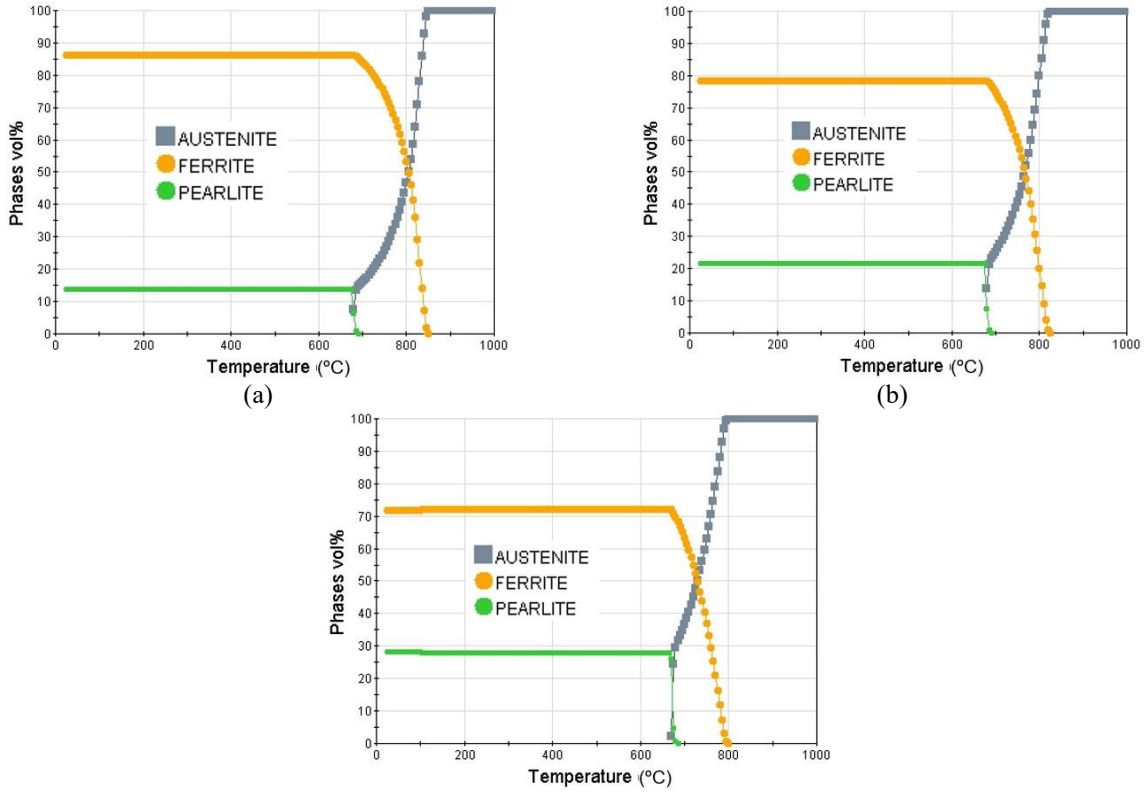

Figure 2. The phase fractions of the initial microstructure were calculated using JMatPro software based on the chemical composition for (a) S235JR, (b) S275JR, and (c) S355JR

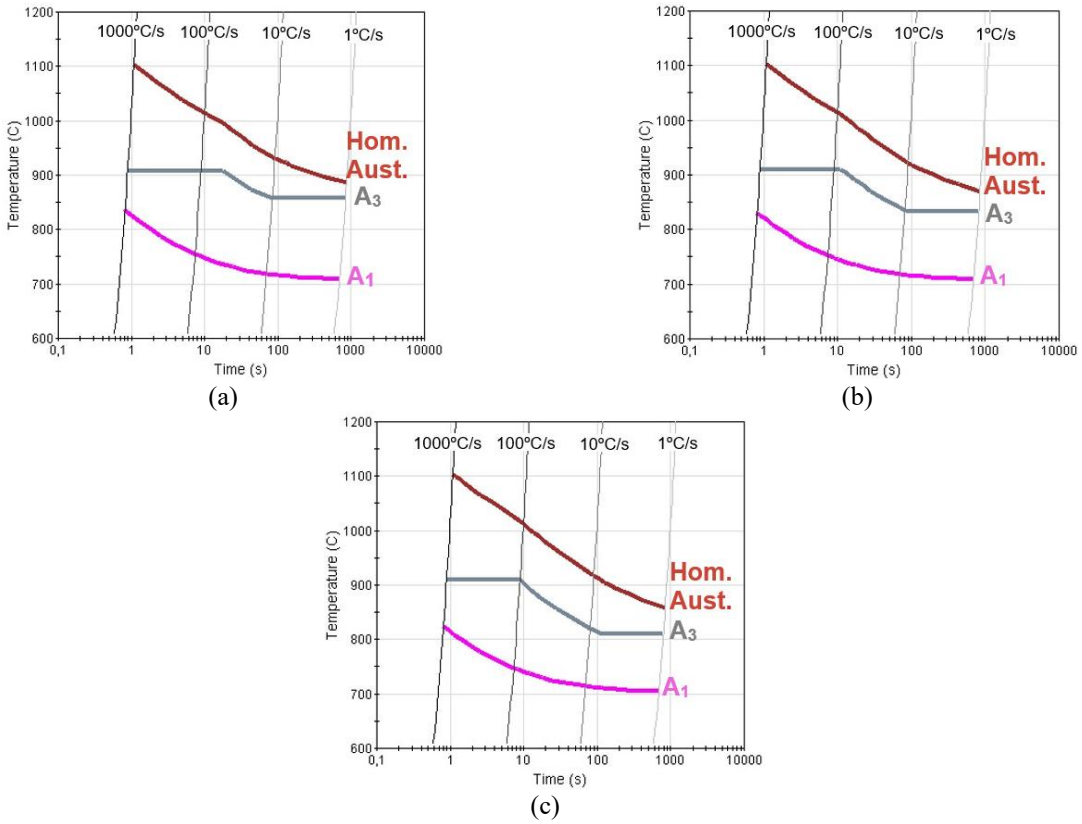

Figure 3. TTA diagram was calculated using JMatPro software for (a) S235JR, (b) S275JR, and (c) S355JR

steels were 858.4°C, 833.3°C and 810.3°C respectively. This decrease in the transformation temperature is due to the increase in the ratio of carbon and alloying elements. The austenite phase is more stable with increasing carbon content, which delays ferrite transformation [21]. Carbon atoms interfere with the nucleation and growth processes of the ferrite phase, making diffusion difficult, which reduces the transformation temperature [21]. Due to the increasing carbon content, the martensitic transformation starts (Ms), and end (Mf) temperatures of structural steels also decrease. The martensitic transformation starting temperatures of S235JR, S275JR and S355JR were calculated as 469.9°C, 438.7°C and 404.8°C, respectively. This is a known behavior that the amount of carbon in the composition of steels makes austenite more stable and thus reduces the martensite starting temperature [21]. Increasing the carbon content slows down the kinetics of martensite transformation, causing transformation to start at lower temperatures [21]. The bainite transformation curves shift to the right on the time axis from S235JR to S355JR, indicating that bainite transformation occurs more slowly. This trend clearly shows that bainite transformation takes longer time in steels with higher carbon and alloying elements [14]. Especially in S355JR steel, the later onset of bainite transformation indicates that the bainite nucleation process takes longer due to the increased alloying element content. The slowing of bainite transformation is due to the reduced diffusion of carbon in the austenite phase, which delays the transformation kinetics [14].

These transformations directly affect the microstructure and mechanical properties of steels. For example, the slower formation of bainite in S355JR can increase the hardness and strength of this steel while potentially reducing its ductility. Understanding these transformation behaviors, as shown in TTT diagrams, plays a critical role in optimizing heat treatment processes for structural steels. By controlling cooling rates and transformation temperatures, the microstructure can be adjusted to achieve desired hardness, strength, and toughness properties.

Most heat treatments are related to transformations that occur during continuous cooling [16]. Since TTT diagrams show the time-temperature relationship of austenitic transformation at constant temperature, the curves showing the cooling rate theoretically do not coincide with the curves in the TTT diagram. In addition, it is known that with the effect of continuous cooling, the nose of the transformation curves in the CCT diagram shifts down and to the right according to the position of the isothermal transformation curves [19]. Hence, it is more accurate to use the CCT diagram in the investigation of phase transformations with cooling rate. Therefore, the temperature values recorded during the cooling of the samples (experimental cooling rate) can be applied to the continuous cooling transformation diagrams created with the JMatPro software to examine possible microstructural features. Figure 5 is the continuous cooling transformation diagrams of structural steels austenitized at 1000ºC and the experimental cooling rate of these steels is shown by the dashed line. The cooling rates of S235JR, S275JR and S335JR structural steels between 500ºC-800ºC were 33ºC/s, 27ºC/s and 26ºC/s respectively. It can be seen that the transformation curves in the CCT diagram (Figure 5 (a) to (c)) also shift downward and to the right with the increase in the carbon content in the chemical composition of the structural steels. The cooling curves of all three steels do not intersect the martensitic transformation region and only intersect the ferrite and bainite transformation regions. Therefore, ferrite and bainite phases are expected to form in the microstructure of all three steels. Although S235JR exhibits a slightly higher cooling rate, the austenite-ferrite transformation started at higher temperatures (about 800ºC) compared to the other two structural steels. In addition, the experimental cooling curve of S235JR crosses the ferrite transformation zone more. Therefore, more ferrite phases are expected to form in the microstructure of S235JR steel compared to the other two structural steels. With increasing carbon content in the structural steels (from S235JR to S355JR), the region between the ferrite transformation initiation curve and the bainite transformation initiation curve narrows and the distance at which the experimental cooling curves intersect the two transformation curves decreases.

This indicates that the possible ferrite phase fraction from S235JR to S355JR will decrease and the bainite phase fraction will increase. Increasing bainite phase fraction in the microstructure of these steels means that the hardness will increase. As a matter of fact, the experimental hardness of S235JR, S275JR and S335JR were determined as 224$HV_{0.3}$, 275$HV_{0.3}$ and 345$HV_{0.3}$, respectively (Table 2). In addition, the estimated hardness values of JMarPro showed great consistency with the experimental hardness values (Figure 5 (a) to (c)).

Table 2. Microhardness values structural steels before and after heat treatment

Structural Steels	Base hardness $HV_{0.3}$	Heat treatment hardness $HV_{0.3}$
S235JR	140	224
S275JR	165	275
S355JR	185	345

Figure 6 shows the microstructural details of S235JR, S275JR and S355JR steels after air cooling heat treatment. Optical microscope images of the structural steels show the presence of Primary Ferrite (PF), Ferrite/Carbide Aggregate (FCA), Widmanstätten Ferrite (WF) and Bainite (B) structures (Figure 6(a)-(c)). PF is formed by nucleation of ferrite along pre-existing austenite grains, usually at elevated temperatures, and is observed as equilateral or polygonal grains formed by slower cooling and diffusion-controlled processes [18].

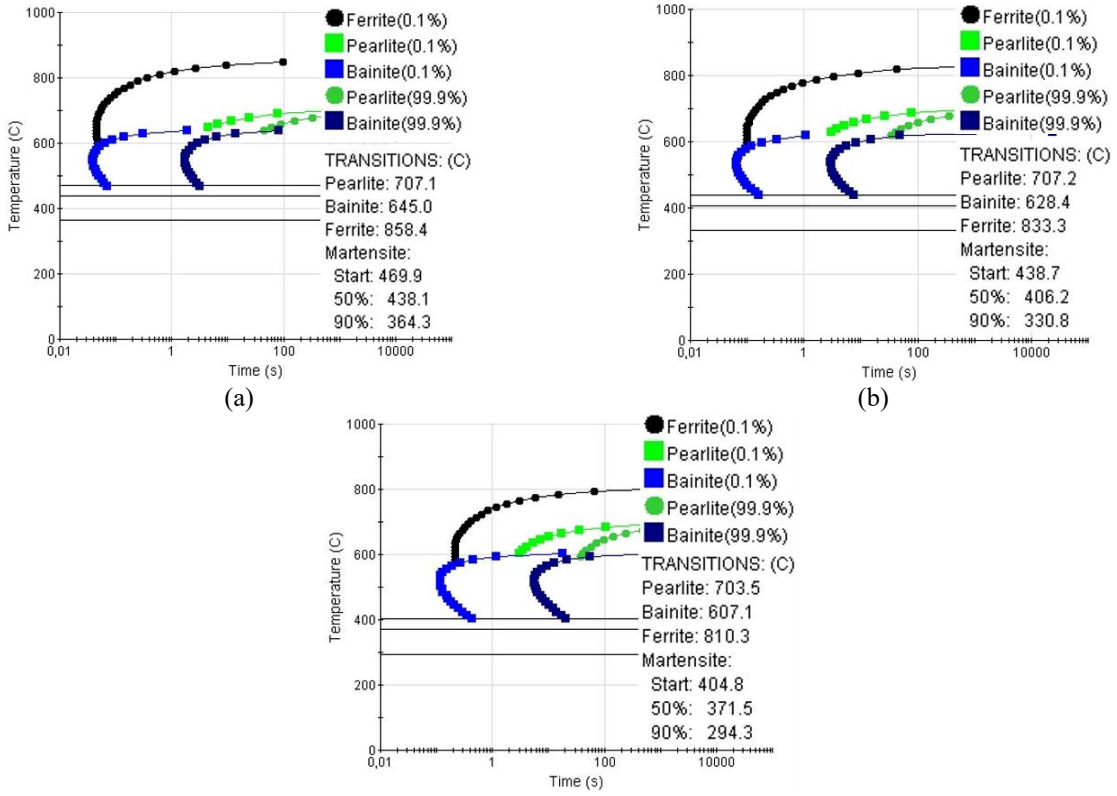

Figure 4. TTT diagram was calculated using JMatPro software for (a) S235JR, (b) S275JR, and (c) S355JR

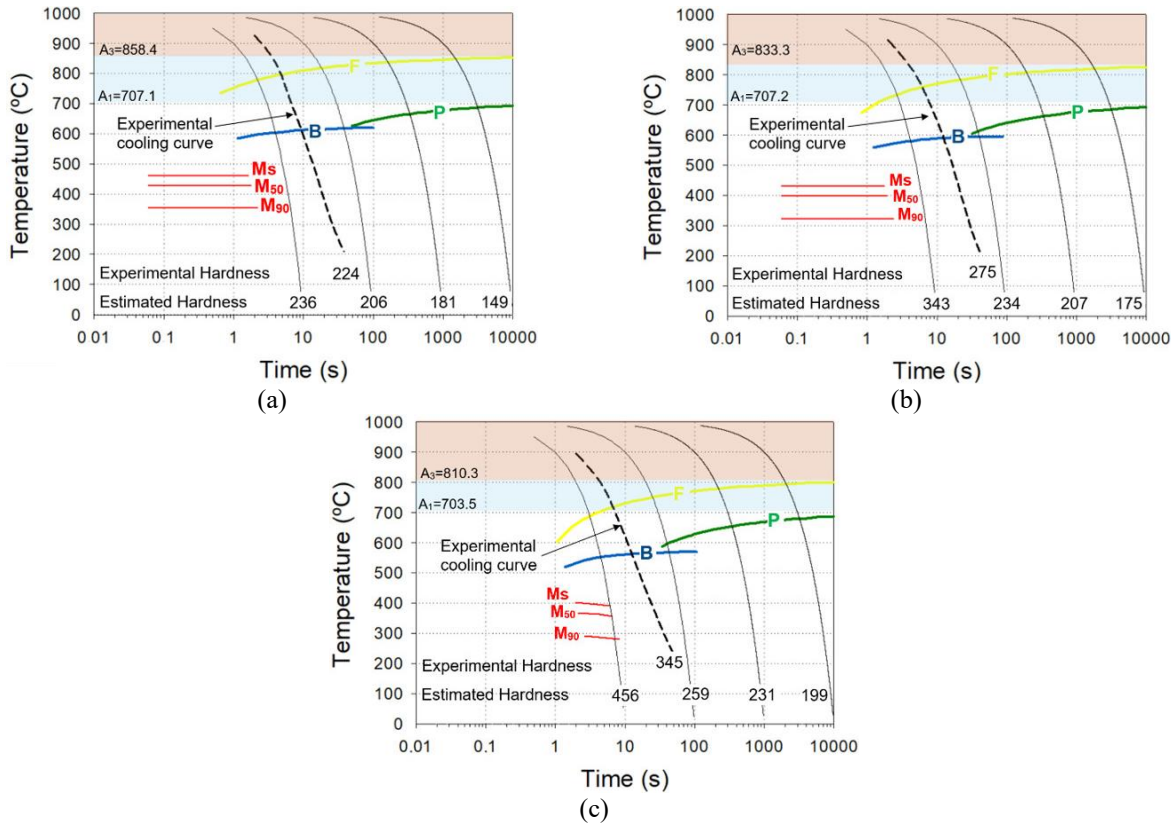

Figure 5. JMatPro predictions of CCT diagram for the present (a) S235JR, (b) S275JR, and (c) S355JR steels austenitized at 1000 °C

FCA is a unique microstructure that occurs in low carbon manganese steels under continuous cooling conditions between pearlite and bainite formation temperatures; unlike pearlite or bainite, it consists of a smooth ferrite matrix containing finely dispersed cementite particles [16]. WF nucleates at a lower subcooling temperature and grows as thin, elongated plates extending from austenite grain boundaries or inclusions and has high aspect ratios and appears in a colony structure of parallel plates [18].

Bainite forms by a displacive transformation at lower temperatures and grows as individual plates or slopes; in upper bainite carbides are deposited between ferrite plates, while in lower bainite they are precipitated both within and between ferrite plates [14]. These microstructures are formed under different temperatures and cooling conditions and are distinguished from each other by their transformation mechanisms and morphology. From S235JR to S355JR, the PF structure in the microstructure of the structural steels decreases and the WF plates become thinner (Figure 6(a2) -(c2)). From S235JR to S275JR, the WF and FCA structure increases (Figure 6(a2) -(b2)). From S275JR to S355JR, B structure increases while WF decreases (Figure 6(b2) -(c2)). While WF and PF structures can be directly distinguished as ferrite phase by thresholding, B and FCA are very difficult to distinguish. Therefore, these two phases are referred to as "others" in Figure 6(a2) -(c2). Figure 6 (a2) to (c2) shows that the fraction of ferrite phase decreases and the fraction of FCA and B increases. These experimentally observed microstructural features are in agreement with the transformation characteristics in the CCT diagrams given in Figure 5. The PF and WF fraction of 52% in structural steel (0.17%C, 0.52%Mn), cooled from 1100ºC at a cooling rate of 25ºC/s as reported by Martino et al. [22], is consistent with the PF and WF fraction of 49% at a cooling rate of 33ºC/s observed in S235JR steel in the present study (Figure 6 (a2)). The PF and WF fraction of 36% in S275JR steel cooled at a rate of 27ºC/s is comparable to the PF and WF fraction of 43% at a 25ºC/s cooling rate in another structural steel (0.17%C, 1.86%Mn) [22]. In the microstructure of S355JR steel, 30% PF and WF were detected (Figure 6 (a2)).

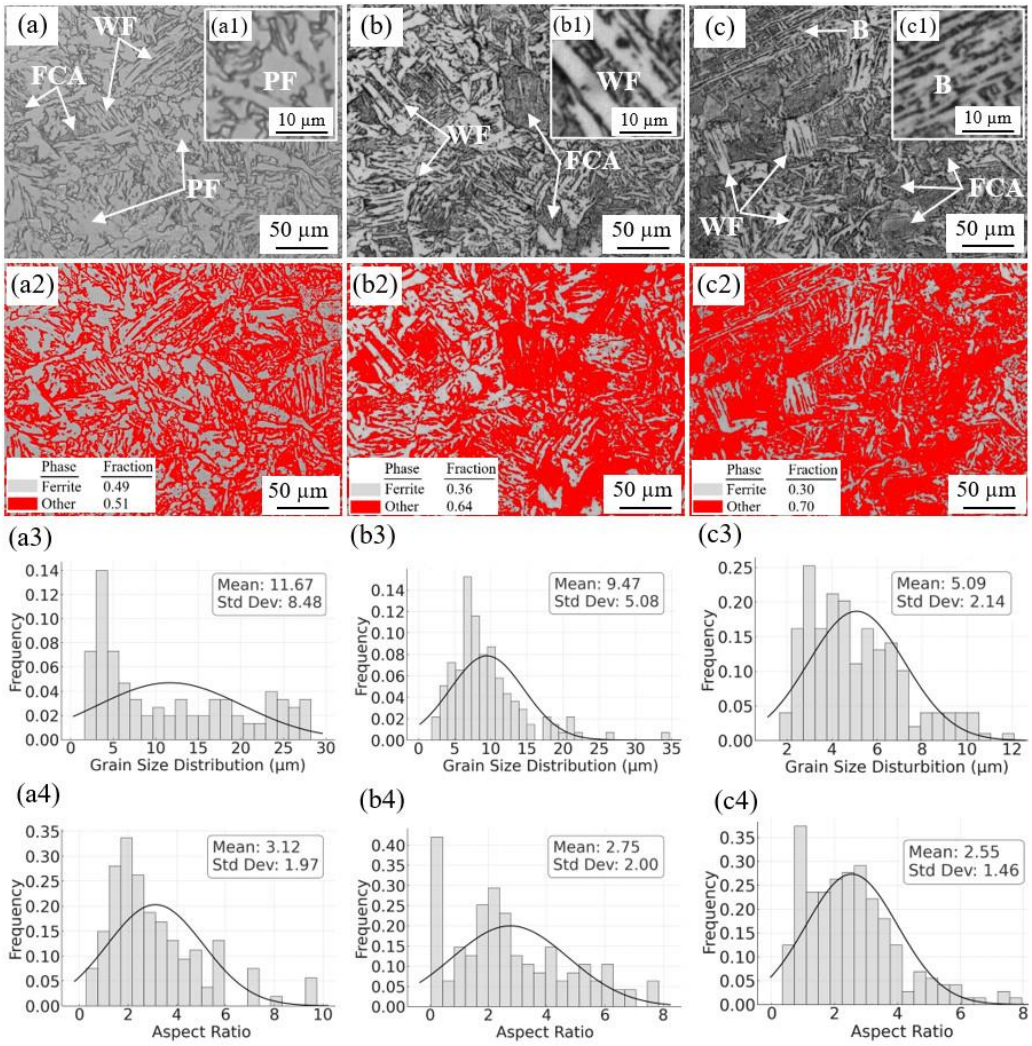

Figure 6. Optical microscope images, phase maps, grain size distributions, and aspect ratios of the microstructures of (a)-(a4) S235JR, (b)-(b4) S275JR, and (c)-(c4) S355JR following heat treatment (PF: Primary Ferrite, FCA: Ferrite/Carbide Aggregate, WF: Widmanstätten Ferrite, B: Bainite)

This indicates that the increased C and Mn content leads to the formation of more B and FCA in the microstructure. The average ferrite grain size of S235JR steel was 11.67 µm and aspect ratio was 3.12 (Figure 6(a3) and (a4)); the average ferrite grain size of S275JR steel was 9.47 µm and aspect ratio was 2.75 (Figure 6(b3) and (b4)); the average ferrite grain size of S355JR steel was 5.09 µm and aspect ratio was 2.55 (Figure 6(c3) and (c4)). Figure 7 illustrates the effect of heat treatment on the grain size of structural steels. Increasing C and Mn content in steels delays the transformation of the austenite phase to ferrite, resulting in the formation of more nucleation points, which reduces the size and aspect ratio of ferrite grains [23]. Carbon lowers the transformation temperature and promotes the formation of finer ferrite grains, while manganese stabilizes the austenite phase, increasing the nucleation rate and limiting dislocation movement [24,25].

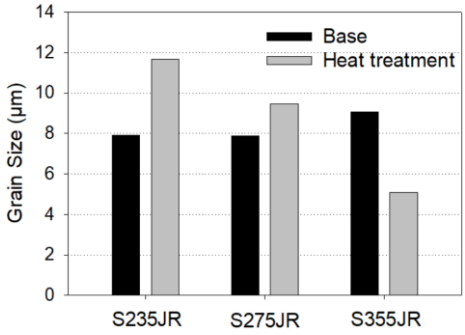

Figure 7. Grain size graph of structural steels before and after heat treatment

Furthermore, an increased proportion of these elements forms carbide precipitates in the ferrite phase and accumulates at grain boundaries, physically limiting the growth of grains [26]. The combination of these effects explains the formation of a finer grained and decreasing aspect ratio structure in the ferrite phase from S235JR to S355JR. In addition, the increase in bainite content and reduction in ferrite grain size in the microstructure of these structural steels following heat treatment contribute to the observed hardness increase.

JMatPro predictions of the phases that will form in the microstructure of structural steels according to cooling rates are given in Figure 8. The experimental cooling rates of these steels are shown with a dashed line in the phase fraction-cooling rate graph. According to these graphs, approximately 46% ferrite and 0.54 bainite (Figure 8(a)) in the microstructure of S235JR steel, approximately 38% ferrite and 0.62 bainite (Figure 8(b)) in the microstructure of S275JR steel, approximately 30% ferrite and 0.70 bainite (Figure 8(c)) in the microstructure of S355JR steel. The estimated perlite fraction is neglected because it is too low (0.001%-0.004%). Also, no pearlite was observed in the microstructure examinations. The prediction of the phase fractions in Figure 8 showed high consistency with the phase fractions determined from the microstructure investigations (Figure 6(a2) -(c2)) with a maximum deviation of 3%. These findings show that JMatPro predictions are in agreement with the experimental results and can reliably predict the microstructure phase fractions of structural steels due to cooling rates.

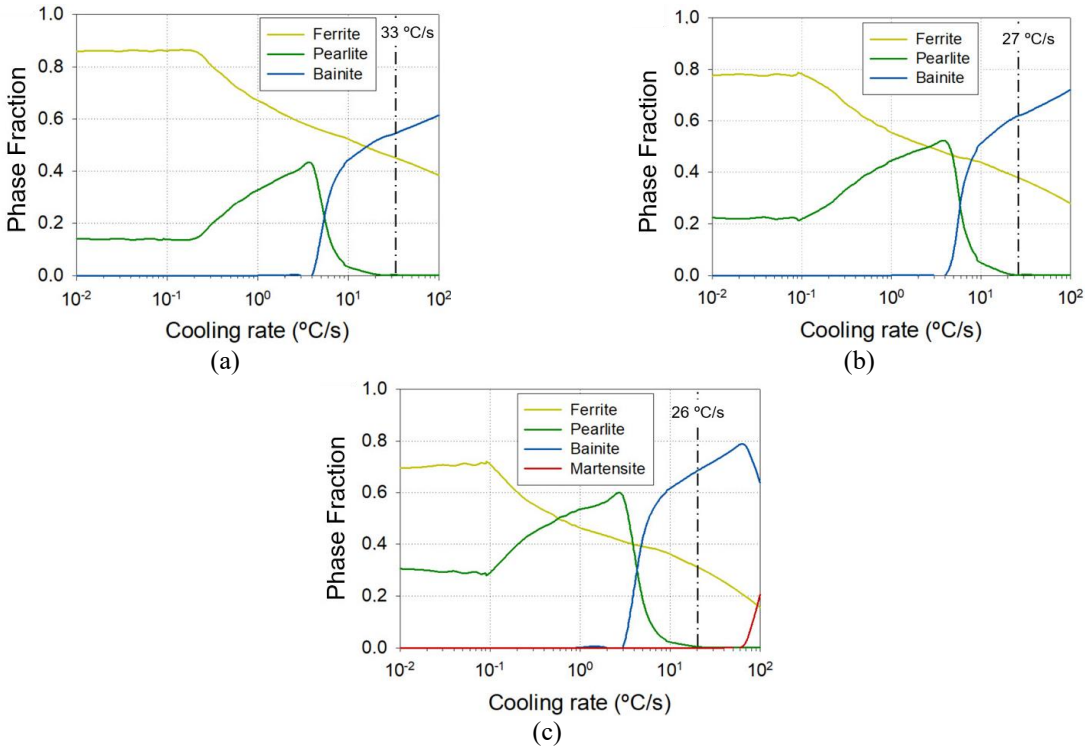

Figure 8. JMatPro simulations illustrate the changes in phase fractions of (a) S235JR, (b) S275JR, and (c) S355JR based on cooling rates from the austenitization at 1000ºC

4 Conclusions

In this study, the phases, phase fractions, and hardness values of S235JR, S275JR, and S355JR structural steels after air-cooling heat treatment were analyzed using both experimental methods and material property simulation software. The principal findings are presented below.

1. An increase in the carbon and manganese content of structural steels results in a progressive reduction in transformation temperatures, which can be attributed to the enhanced stability of the austenite phase.
2. The presence of higher carbon and manganese fractions results in a downward and rightward shift of the ferrite and austenite transformation curves, thereby causing transformations to occur at lower temperatures over longer periods. This shift results in a reduction in ferrite grain size, an increase in the bainite phase fraction, and a consequent rise in hardness.
3. The microstructure of the structural steels was validated through experimental observations, as predicted by the intersection of the ferrite and bainite regions in the CCT (Continuous Cooling Transformation) diagrams of the experimental cooling curves. Furthermore, the hardness values predicted by the CCT diagrams were found to be in agreement with the experimentally measured values.
4. The experimental results revealed deviations of less than 3% between the phase fractions predicted by JMatPro software and those determined via microstructural analysis. This confirms the software's reliability in accurately predicting the effects of cooling rates on steel microstructures under slow cooling conditions.

Conflict of interest

The authors declare that there is no conflict of interest.

Similarity rate (iThenticate): 16 %

References

[1] Y. Li, M. Wang, G. Li and B. Jiang, Mechanical properties of hot-rolled structural steels at elevated Temperatures: A review. Fire Safety Journal, 119, 1-23, 2021. https://doi.org/10.1016/j.firesaf.2020.103237.

[2] D.A. Fadare, T.G. Fadara and O.Y. Akanbi, Effect of Heat Treatment on Mechanical Properties and Microstructure of NST 37-2 Steel. Journal of Minerals and Materials Characterization and Engineering. 10 299–308, 2011. https://doi.org/10.4236/jmmce.2011.103020.

[3] B. Sun, A.K. da Silva, Y. Wu, Y. Ma, H. Chen, C. Scott, D. Ponge and D. Raabe, Physical metallurgy of medium-Mn advanced high-strength steels. International Materials Reviews. 68, 786–824, 2023. https://doi.org/10.1080/09506608.2022.2153220.

[4] M.M. Solomon, S.A. Umoren, A. Gilda Ritacca, I. Ritacco, D. Hu and L. Guo, Tailoring poly (2-ethyl-2-oxazoline) towards effective mitigation of chloride-induced dissolution of S235JR steel: The synergistic contributions of potassium iodide and myristyl trimethylammonium bromide. Journal of Molecular Liquids, 396, 1–21, 2024.https://doi.org/10.1016/j.molliq.2023.123935.

[5] A.K. Krella, D.E. Zakrzewska and A. Marchewicz, The resistance of S235JR steel to cavitation erosion. Wear, 452–453, 1–14, 2020. https://doi.org/10.1016/j.wear.2020.203295.

[6] G. İrsel, Study of the microstructure and mechanical property relationships of shielded metal arc and TIG welded S235JR steel joints. Materials Science and Engineering: A, 830, 1–14, 2022. https://doi.org/10.1016/j.msea.2021.142320.

[7] M. Gamerdinger, F. Akyel, S. Olschok and U. Reisgen, Investigating mechanical properties of laser beam weld seams with LTT-effect in 1.4307 and S235JR by tensile test and DIC. Procedia CIRP, 111- 420–424, 2022. https://doi.org/10.1016/j.procir.2022.08.179.

[8] A. Neimitz and J. Galkiewicz, The experimental-numerical analyses of the failure mechanisms of S355JR steel, Theoretical and Applied Fracture Mechanics. 108, 1–14, 2020. https://doi.org/10.1016/j.tafmec.2020.102666.

[9] N. Torić, J. Brnić, I. Boko, M. Brčić, I.W. Burgess and I.U. Glavinić, Development of a high temperature material model for grade s275jr steel. Journal of Constructional Steel Research, 137, 161–168, 2017. https://doi.org/10.1016/j.jcsr.2017.06.020.

[10] Q. Chen, J. Yang, X. Liu, J. Tang and B. Huang, Effect of the groove type when considering a thermometallurgical-mechanical model of the welding residual stress and deformation in an S355JR-316L dissimilar welded joint. Journal of Manufacturing Processes, 45, 290–303, 2019. https://doi.org/10.1016/j.jmapro.2019.07.011.

[11] W. Yongzhong and Z. Donghui, Electrochemical corrosion behaviors and microhardness of laser thermal sprayed amorphous AlCrNi coating on S275JR steel. Optics & Laser Technology Journal, 118, 115–120, 2019. https://doi.org/10.1016/j.optlastec.2019.05.004.

[12] Y. Tomita and K. Okabayashi, Effect of microstructure on strength and toughness of heat-treated low alloy structural steels. Metallurgical and Materials Transactions A, 17, 1203–1209, 1986. https://doi.org/10.1007/BF02665319.

[13] L.A. Dobrzański and R. Honysz, Heat treatment influence on mechanical properties of structural steels for quenching and tempering. Journal of Achievements in Materials and Manufacturing, 55, 461–468, 2012.

[14] P. Chakraborty, S. Neogy, N.K. Sarkar, H. Donthula, S.K. Ghosh, H.K. Nandi, B. Gopalakrishna, I. Balasundar and R. Tewari, Formation of Bainite in a Low-Carbon Steel at Slow Cooling Rate – Experimental Observations and Thermodynamic Validation. Steel Research International, 2400593, 1–12 2024. https://doi.org/10.1002/srin.202400593.

[15] F.X. Ding, L.F. Lan, Y.J. Yu and M.K. Man, Experimental study of the effect of a slow-cooling heat treatment on the mechanical properties of high strength steels. Construction and Building Materials, 241, 1–12, 2020. https://doi.org/10.1016/j.conbuildmat.2020.118020.

[16] S.F. Di Martino and G. Thewlis, Transformation characteristics of ferrite/carbide aggregate in continuously cooled, low carbon-manganese steels. Metallurgical and Materials Transactions A. 45, 579–594, 2014. https://doi.org/10.1007/s11661-013-2035-x.

[17] A. Thakur and G.-E. Aregawi, International Journal of Current Engineering and Technology Effect of Heat Treatment on Mechanical Properties and Microstructure of ST 37-2 Rear Trailing Arm (Case study at MIE). International Journal of Current Engineering and Technology, 9, 80–90, 2019. https://doi.org/10.14741/ijcet/v.9.1.12.

[18] G. Thewlis, Classification and quantification of microstructures in steels Materials Science and Technology, 20, 143–160, 2004. https://doi.org/10.1179/026708304225010325.

[19] J.S. Kirkaldy and D. Venugopolan, Phase Transformations in Ferrous Alloys. International Conference on Phase Transformations in Ferrous Alloys, pp. 125–125, Philadelphia, USA, 1984.

[20] J.S. Kirkaldy, Diffusion-controlled phase transformations in steels. Theory and applications, Scandinavian Journal of Metallurgy, 20, 50–61, 1991.

[21] J. Rezaei, M. Habibi Parsa and H. Mirzadeh, Phase transformation kinetics of high-carbon steel during continuous heating. The Journal of Materials Research and Technology, 27, 2524–2537, 2023. https://doi.org/10.1016/j.jmrt.2023.10.089.

[22] S.F. Di Martino and G. Thewlis, Transformation Characteristics of Ferrite/Carbide Aggregate in Continuously Cooled, Low Carbon-Manganese Steels. Metallurgical and Materials Transactions A, 45, 579–594, 2014. https://doi.org/10.1007/s11661-013-2035-x.

[23] V.L. de la Concepción, H.N. Lorusso and H.G. Svoboda, Effect of Carbon Content on Microstructure and Mechanical Properties of Dual Phase Steels. Procedia Materials Science, 8, 1047–1056, 2015. https://doi.org/10.1016/j.mspro.2015.04.167.

[24] A.N. Ashong, M.Y. Na, H.C. Kim, S.H. Noh, T. Park, H.J. Chang and J.H. Kim, Influence of manganese on the microstructure and mechanical properties of oxide-dispersion-strengthened steels. Materials and Design, 182, 1–13, 2019. https://doi.org/10.1016/j.matdes.2019.107997.

[25] I. Pushkareva, J. Macchi, B. Shalchi-Amirkhiz, F. Fazeli, G. Geandier, F. Danoix, J.D.C. Teixeira, S.Y.P. Allain and C. Scott, A study of the carbon distribution in bainitic ferrite, Scripta Materialia. 224, 1–5, 2023. https://doi.org/10.1016/j.scriptamat.2022.115140.

[26] M. Calcagnotto, D. Ponge and D. Raabe, On the Effect of Manganese on Grain Size Stability and Hardenability in Ultrafine-Grained Ferrite/Martensite Dual-Phase Steels. Metallurgical and Materials Transactions A, 43, 37–46, 2012. https://doi.org/10.1007/s11661-011-0828-3.